Identification of Open-Circuit Faults in T-Type Inverters Using Fuzzy Logic Approach

Amina MIMOUNI[1] , Souad LARIBI[1] , Tayeb ALLAOUI[1] , Morsli SEBAA[1] ,
Abdelkader Azzeddine BENGHARBI[1]

[1]Laboratory of Energy Engineering and Computer Engineering,Ibn Khaldoun University,
BP 78, Tiaret, Algeria

amina.mimouni@univ-tiaret.dz, souad.laribi@univ-tiaret.dz, tayeb.allaoui@univ-tiaret.dz,
m_sebaa@univ-tiaret.dz, bengharbi.aek.azz@univ-tiaret.dz

Abstract. *With the increasing adoption of solar Photovoltaic (PV) systems in several applications, reliability and service continuity are important challenges that need to be addressed. Power converters are vital components in solar PV systems and inverters tend to be the most likely devices of equipment to experience faults which usually occur in the switching devices. It is therefore critical to assess the functioning of the inverters and identify these faults in order to lower risks and the resulting financial losses. Open-circuit faults (OCF) are among the most common. This paper suggests a fuzzy-based fault detection approach for the T-Type inverter in grid connected PV system based on the diagnosis variables which are calculated using the average values of positive and the negative parts of the normalized output currents data. After that, these variables are analyzed using a fuzzy logic technique, The single, multiple power switch open circuit faults may all be detected and diagnosed utilizing this fuzzy-based fault diagnostic technique. The results of the simulation in MATLAB show that the proposed method can accurately identify and locate OCF the inverter switches.*

Keywords

Grid connected PV system, T-Type inverter, Fault diagnosis, Open Circuit Fault, Fuzzy logic approach.

1. Introduction

The demand for global electricity continues its persistent growth, serving both domestic and industrial needs. However, this heightened demand relies predominantly on fossil fuels like coal, natural gas, and oil for electricity generation. Unfortunately, the world's reserves of these resources are rapidly depleting, compounded by their adverse environmental consequences including pollution and global warming [1, 2].

Analyzing the data from 2010 to 2019 regarding carbon dioxide (CO_2) emissions linked to global energy production from the power sector reveals a significant pattern. Starting at 30.4 Gt in 2010, these emissions increased to 31.3 Gt in 2011 and continued to rise in subsequent years: 2012 (31.6 Gt), 2013 (32.2 Gt), and 2014 (32.3 Gt). Emissions then remained steady in 2015 and 2016 at 32.2 Gt, followed by a climb to 32.7 Gt in 2017, and ultimately reaching 33.3 Gt in both 2018 and 2019 [3]. This disconcerting pattern has prompted a gradual shift towards adopting cleaner, sustainable, and economically viable alternative energy sources. The driving force behind this shift is a significant reduction in CO_2 emissions, especially in advanced economies. Notably, within these advanced economies, the total CO_2 emissions have decreased by over 3.2 %, equivalent to a reduction of around 370 million metric tons of CO_2. Importantly, the power sector has played a major role in achieving this decline, accounting for a substantial 85% of this accomplishment. This achievement highlights the profound impact of significant modifications in electricity generation methodologies on the substantial attenuation of CO_2 emissions [4].

Over the past decade, the deployment of solar Photovoltaic (PV) around the world has massively increased. The PV market expansion was essentially driven by a lower production costs and supportive policies from local governments. These incentives are making solar installations' Return on Investment (ROI) appear more attractive [5, 6, 7]. Like all other industrial processes, a PV system is susceptible to a variety of faults and anomalies that can affect its performance or even make it completely inoperable. All these negative effects will undoubtedly lower the installation's productivity and consequently, its profit. Not to mention the maintenance cost to get the system back to normal operation [8, 9]. The reliability, safety, and quality of the energy produced can be significantly impacted by inverters, which are at the core of the PV system. Therefore, inverters must meet increased reliability requirements, which remain crucial for highly efficient energy conversion [10].

Recent energy challenges have stimulated the development of new power electronic converter topologies and technological improvement of semiconductor devices to handle the increasing power demand. Multilevel inverters (MLIs) have proven superior performance over the conventional two-level (2L) topologies for wide output power ranges, and they are being widely in a variety of applications, including renewable energy systems. These topologies increase the inverter's power capacity and enhance the quality of energy by reducing the level of harmonics. In addition, they allow low voltage ratings of the components and reduces the output grid filter [11, 12]. There are several MLI topologies used in grid-tied PV installations. The T-type three-level (3L) inverter topology has received the most attention among the existing topologies. The main benefits of T-type topology are the elimination of clamping diodes and flying capacitors and the reduction of conduction losses in the power switches [13, 14].

With regard to continuity of service, inverters are particularly sensitive to faults in their power switches. An (OCF) or short-circuit fault (SCF) in a power switch can cause serious system malfunctions. Any fault that is not detected can quickly damage the entire power converter stage and auxiliary circuits. Once a fault has occurred, it must be quickly detected to prevent it from spreading to other system's components. Therefore, the implementation of efficient and fast methods of fault detection is imperative [8, 15].

The behavior of the inverters under an OCF of a power semiconductor fault, have been the subject of extensive research and several solutions have been proposed to detect faults and overcome the impact of subsequent failures on the overall system. In [8], the behavior of the measured output current and dc-link capacitor voltages of grid-tie T-Type inverter was analyzed in healthy and faulty operation to design a fuzzy

rule base for the proposed fuzzy logic-based fault detection approach. In [15, 16], the authors presented a diagnosis method based on bridge voltages for a T-type 3L inverter. An OCF detection method for the T-type 3L inverter using the two separate fault signals that are acquired was presented in [16]. A fault detection method was presented in [17] to identify multiple transistor OCF in a T-type 3L inverter. In the study, state transitions under different failure modes were distinguished using a Finite-State Machine (FSM) recording state transitions and Rough Set Theory (RST). The authors in [18, 19, 20] developed a method for diagnosing an OCF and proposed a fault-tolerant control approach for T-type inverter systems. The method was based on the calculation of the average of the normalized phase current and the change in neutral-point voltage. In [21], a unique fault detection technique of OCF for 3L T-type inverter based on Silicon Carbide (SiC) MOSFET is presented. The main purpose of this method is to detect changes in the dc-bus neutral-point current and compare them to the neutral-point current's expected value during normal operation. Several research studies focusing on the detection and location of OCFs in a Neutral Point Converter (NPC) have been published. In [22, 23], the fault diagnosis of NPC inverter is based on a Neural Network (NN) classification method. The authors in [22] proposed an OCF diagnosis technique for grid-connected NPC inverters which is based on the Independent Component Analysis fault feature extraction and NN classifier. This method is effective and uses only on the phase currents. The authors in [24, 25] presented a fault diagnosis method in PV systems. In [24], six possible fault scenarios in grid connected PV system including the inverter were studied. The approach used was based on the extraction of features from the output currents using Discrete Wavelet Transform (DWT) and the identification is based on NN classification. In [25], Artificial Neural Network (ANN) were used to classify open circuit failures in IGBT power converters for PV systems.

This paper proposes an OCF diagnosis technique for the 3L T-Type inverter in grid-connected PV system. The proposed approach uses the three-phase currents, and the fault diagnosis variables are calculated using the average positive and negative normalized currents. The information on the OCF of the switches can then be obtained by analyzing these variables using fuzzy logic. The proposed fuzzy-based fault diagnostic algorithm provides identification and location of single and multiple power switch OCF.
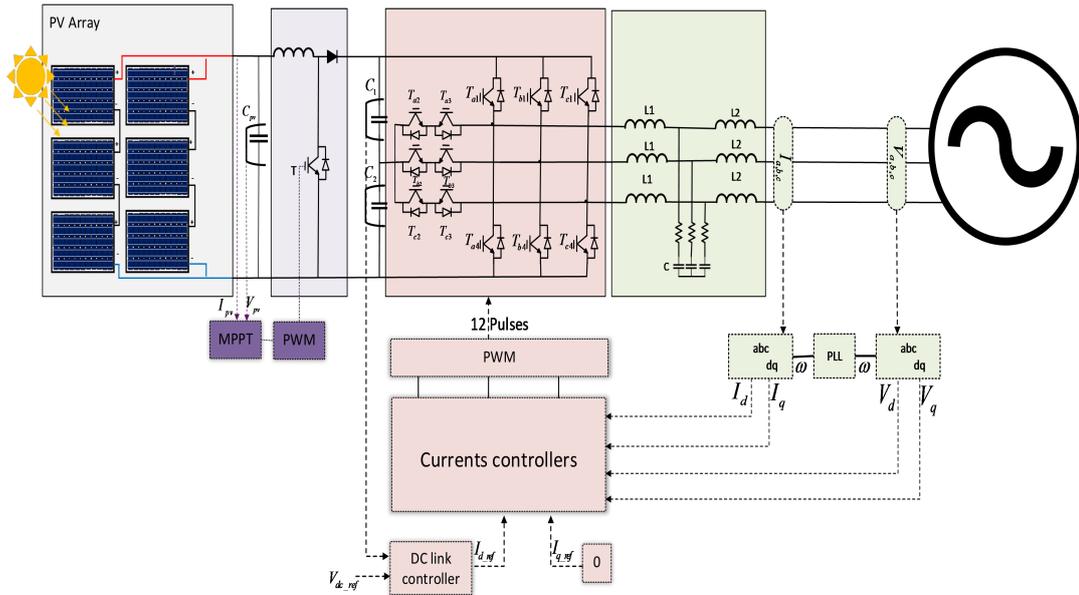
Fig. 1: Schematic of the grid-connected PV system.

2. Modeling of the Studied PV System

To effectively transfer energy from the PV system to the grid, a two-stage grid-connected PV system topology is proposed in this study. Fig. 1 depicts the structure of the system which consists of a PV generator with a DC-DC converter (boost converter) to track the Maximum Power Point (MPP) and a three-level T-Type inverter connected to the grid. The T-type inverter topology offers high quality of energy and low Total Harmonic Distortion (THD).

2.1. PV Cell Model

The PV cell allows the direct conversion of solar energy's radiation into electricity [26]. Several models have been proposed for the PV cell. The one-diode model has often been the most common due to its ease of use and effectiveness in simulating the characteristics of PV cells. This model includes a current source I_{ph} which represents the photogenerated current, A shunt resistance (R_{sh}), and a series resistance (R_s) that reflects the losses in the semiconductor material [26, 27]. Fig. 2 shows the equivalent circuit of the PV cell used in this work.

The output current of a PV cell is given by [27, 28]:

$$I_{pv} = I_{ph} - I_d - I_{sh}, \qquad (1)$$

$$I_{pv} = I_{ph} - I_0 \left(\exp^{\frac{I_{pv} \times R_s + V_{pv}}{V_t}} \right) - \frac{I_{pv} \times R_s + V_{pv}}{R_{sh}}, \quad (2)$$

where I_{ph} represents the light generated current, I_d is the diode current, I_0 is the diode saturation current
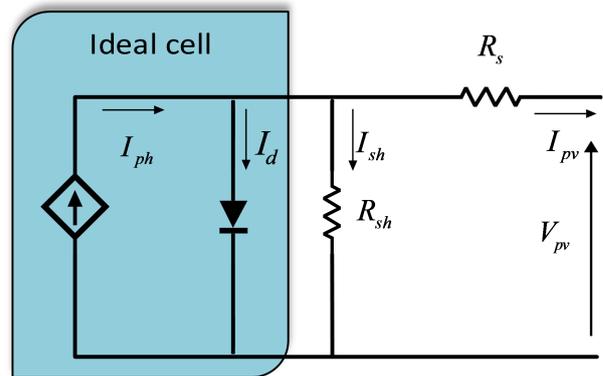

Fig. 2: Equivalent circuit of PV cell.

and I_{sh} is the shunt resistance current. The V_t thermal voltage is given by:

$$V_t = \frac{AKT}{q}, \qquad (3)$$

where A is a diode ideality factor, K represents Boltzmann's constant $(1.38 \times 10^{-23} (J/K))$, and q is the Electron charge $(1.6 \times 10^{-19} C)$.

2.2. MPPT controller design for the DC-DC converter

The power output of the PV generator (GPV) depends on several climatic factors, such as irradiation and temperature. However, real-time tracking of the Maximum Power Point (MPP) is required to optimize the system performance [1, 2]. The MPPT proposed in this paper is based on Adaptive Neuro-Fuzzy Inference Systems (ANFIS).

Fig. 3 depicts PV system with the DC-DC boost converter conversion and the ANFIS-based MPPT control. The PV array is coupled directly to a filtering capacitor.The MPPT algorithm uses only the PV voltage and current measurements to regulate the duty cycle of the boost converter [29, 30].

ANFIS technique combines ANN learning ability with fuzzy inference system (FIS). The suggested AN-FIS controller's inputs are identical to those of a fuzzy controller, which are the error, the variation of the error, and a single output called the variation of the duty cycle. The two input variables are determined using the error E and the change of error dE given by equations (4) and (5), respectively. The boost converter is driven by the duty ratio at the output, which enables the PV to be operated at its peak power [31, 32].
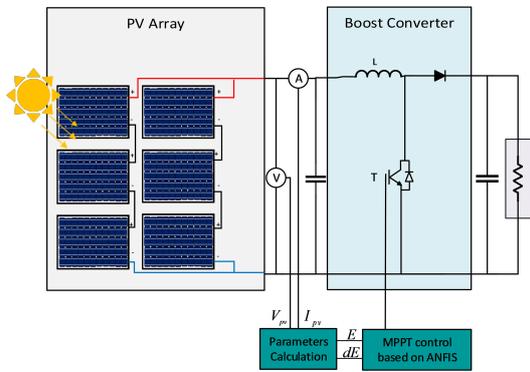

Fig. 3: PV system with ANFIS-based MPPT controller.

$$E(k) = \frac{P_{pv}(k) - P_{pv}(k-1)}{V_{pv}(k) - V_{pv}(k-1)}. \tag{4}$$

$$dE(k) = E(k) - E(k-1), \tag{5}$$

where $P(k)$ and $P(k-1)$ represent the current and previous values of the measured PV output power respectively, $V(k)$ and $V(k-1)$ refer to the measured current and previous PV output voltage respectively.

The structure of ANFIS model is presented in Fig. 4 The number of epochs used for training ANFIS is 2000 and the membership functions for input variables E and dE are 4 shown in Fig. 4, Hence, there are 16 rules all together. The results of this approach provide a very accurate calculation of the GPV's maximum power.

2.3. Three Phase T-Type inverter

As the use of grid-connected PV system has become more widespread due to environmental concerns, the significance of efficient energy conversion via voltage source inverters (VSI) has increased. The superior performance and wider applicability of MLIs have made them favorable over conventional 2L inverters [12].
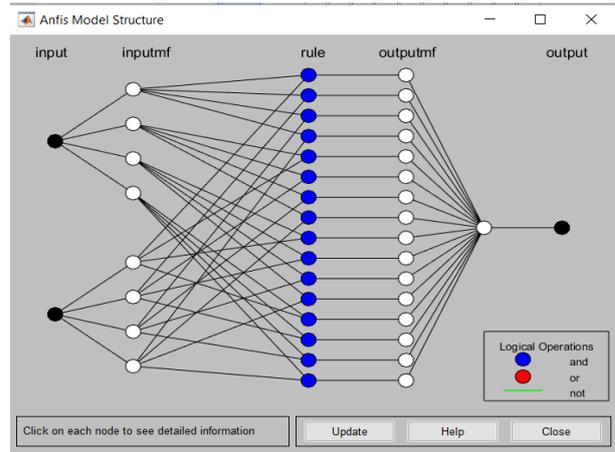

Fig. 4: PV system with ANFIS-based MPPT controller.

There have several MLI topologies proposed in the literature. MLIs can generate a waveform with more than 2L will be a typical feature. This feature reduces THD and increases efficiency compared to a 2L inverter. The most popular topologies are the Neutral Point Clamped (NPC), the Flying Capacitor (FC) and the Cascaded H-bridge (CHB). A T-Type inverter is derived from the traditional NPC with less passive components to offer a smaller size to implement and to mitigate the drawbacks of 3L T-Type NPC MLI. T-Type topologies also benefit from the advantages of two converters, such as low power losses and simple operation, and 3L inverters, such as enhanced efficiency and smoother output voltage waveforms [11, 13, 14].

The fundamental structure of a 3L T-Type inverter is shown in Fig. 5. The conventional 2L VSI design is extended with the addition of an active, bidirectional switch to the dc-link midpoint. The three switching states [P], [N], and [O] that correspond to the three inverter output voltages $+V_{dc}/2$, $-V_{dc}/2$, and 0 can be used to describe the main concept of this inverter in Tab. 1[11].

Tab. 1: Possible states of the 3L T-Type inverter.

Commutation type	T1	T2	T3	T4	V_{AO}
P	ON	ON	OFF	OFF	$+V_{dc}/2$
O	OFF	ON	ON	OFF	0
N	OFF	OFF	ON	ON	$-V_{dc}/2$

- Positive (P) when (T1, T2) are closed.

- Zero (O) when (T2, T3) are closed.

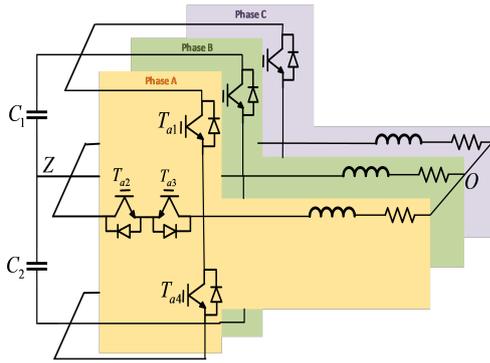- Negative (N) when (T3, T4) switches are closed.

Fig. 5: Structure of a three-phase 3L T-Type inverter.

3. Proposed Fault Diagnosis Method

The use of inverters in grid PV systems has raised awareness to the urgent need to address reliability and service continuity. The power switches are among the most vulnerable devices in the inverter circuit. They play a crucial role in maintaining the reliability of T-Type inverter systems. Therefore, T-Type inverter condition monitoring and fault diagnostics are necessary to reduce the risk of failures and economic losses caused by faults [8, 15].

There are two distinct types of inverter switch faults: SCF and OCF. Power device SCF can happen very quickly and are destructive. Therefore, hardware protection circuits should be able to detect SCFs and provide system protection. OCFs, on the other hand, do not cause the system's breakdown, but lead to performance degradation. However, if this type of failure remains undetected for a long time, this might result in unexpected system damage because it can put healthy transistors under too much stress [16, 17].

For the proposed fault diagnosis technique, the average values of the normalized currents are used as input variables, the models for calculating diagnostic variables will be presented. These variables $i_{x.n}^+$ and $i_{x.n}^-$ should be in the range 0.31 and -0.31 when there is no fault. However, under certain operating conditions, the variances are not always exactly 0.31 and - 0.31.

To use this diagnostic technique, a Park's current vector magnitude is first determined from the three-phase current using (6) and (7) .

The magnitude of the Park's current vector is used to determine the normalized currents (8) .The two components of the normalized currents are then divided into two parts: one with positive values calculated from (9) and (10) one with negative values.

$$\begin{cases} i_d = \dfrac{2}{3}i_a - \dfrac{1}{3}\left(i_b + i_c\right) \\ i_q = \dfrac{1}{\sqrt{3}}\left(i_b - i_c\right) \end{cases}. \tag{6}$$

$$i_s = \sqrt{(i_d)^2 + (i_q)^2}. \tag{7}$$

$$i_{x,n} = \frac{i_x}{|i_s|}, x\epsilon(A,B,C). \tag{8}$$

$$i_{x.n}^+ = \begin{cases} i_{x.n} \Leftarrow i_{x.n} > 0 \\ 0 \Leftarrow i_{x.n} \geqslant 0 \end{cases}. \tag{9}$$

$$i_{x.n}^- = \begin{cases} 0 \Leftarrow i_{x.n} > 0 \\ i_{x.n} \Leftarrow i_{x.n} \geqslant 0 \end{cases}. \tag{10}$$

The average values $i_{x.n.av}^+$ and $i_{x.n.av}^-$ are calculated using equations below (11) and (12) over a moving average window [33].

$$i_{x.n.av}^+(t) = \frac{1}{T}\int_{t-T}^{t} i_{x.n}^+(t)\,dt. \tag{11}$$

$$i_{x.n.av}^-(t) = \frac{1}{T}\int_{t-T}^{t} i_{x.n}^-(t)\,dt. \tag{12}$$

The fundamental period is denoted by T, and the inverter leg index is x.

The threshold values I_{av}^{th1+}, I_{av}^{th2+}, I_{av}^{th1-} and I_{av}^{th2-} in this diagnostic method are chosen based on several simulation tests of different possible scenarios. The purpose is to set thresholds that accurately differentiate between normal and faulty behavior of the system being diagnosed. These thresholds values should be chosen to minimize false flags. The accuracy of our diagnostic method relies on carefully chosen threshold values: $I_{av}^{th1+} = 0.28$, $I_{av}^{th2+} = 0.1$, $I_{av}^{th1-} = -0.28$, and $I_{av}^{th2-} = -0.1$. The following expressions can be used to generate fault symptom variables.

$$\mu_x^+ = \begin{cases} LP, i_{x.n.av}^+ > I_{av}^{th1+} \\ MP, I_{av}^{th2+} < i_{x.n.av}^+ \leqslant i_{x.n.av}^+ \\ SP, i_{x.n.av}^+ \leqslant I_{av}^{th2+} \end{cases}. \tag{13}$$

$$\mu_x^- = \begin{cases} LN, i_{x.n.av}^- > I_{av}^{th1-} \\ MN, I_{av}^{th2-} > i_{x.n.av}^- \geqslant i_{x.n.av}^- \\ SN, i_{x.n.av}^- \geqslant I_{av}^{th2-} \end{cases}. \tag{14}$$

where LP = Large Positive, MP = Medium Positive, SP = Small Positive, LN = Large Negative, MN = Medium Negative, SN = Small Negative. The fault indicator variables μ_A^+, μ_A^-, μ_B^+, μ_B^-, μ_C^+ and μ_C^- can combine to generate a fault signature that is associated with an OCF operating mode in the 3L inverter. For example, in phase A, the OCF location and identification is determined using μ_A^+ and μ_A^-. When $\mu_A^+=$

LP and $\mu_A^- =$ LN, then there is no fault, when $\mu_A^+ =$ MP then T2 is the faulty switch, and for $\mu_A^+ =$ SP, the OCF has occurred in T1. Whereas when OCF has occurred in T3, the fault will be detected when $\mu_A^- =$ MN and T4 is detected when $\mu_A^- =$ SN. This fault diagnosis approach can be applied to single-power-switch open-circuit faults as well as the double power switch open-circuit faults as shown Tab. 2.

Tab. 2: Diagnostic variables identification.

Faulty Switch	μ_A^+	μ_A^-	μ_B^+	μ_B^-	μ_C^+	μ_C^-
T1	SP	LN	LP	LN	LP	LN
T2	MP	LN	LP	LN	LP	LN
T3	LP	MN	LP	LN	LP	LN
T4	LP	SP	LP	LN	LP	LN
T5	LP	LN	SP	LN	LP	LN
T6	LP	LN	MP	LN	LP	LN
T7	LP	LN	LP	MN	LP	LN
T8	LP	LN	LP	SN	LP	LN
T9	LP	LN	LP	LN	SP	LN
T10	LP	LN	LP	LN	MP	LN
T11	LP	LN	LP	LN	LP	MN
T12	LP	LN	LP	LN	LP	SN
T1||T4	SP	SN	LP	LN	LP	LN
T5||T8	LP	LN	SP	SN	LP	LN
T9||T12	LP	LN	LP	LN	SP	SN
T1||T8	SP	LN	LP	SN	LP	LP
T1||T12	SP	LN	LP	LN	LP	SN
T4||T5	LP	SN	SP	LN	LP	LN
T4||T9	LP	SN	LP	LN	SP	LN
T5||T12	LP	LN	SP	LN	LP	SN
T8||T9	LP	LN	LP	SN	SP	LN
Healthy	LP	LN	LP	LN	LP	LN

3.1. Fuzzy logic fault diagnosis approach

The operating principle of fuzzy logic-based fault diagnosis is to extract and compute input signals, using fuzzy rules represented as membership functions, which can contain all possible combinations that correspond to the fault mode considered [8, 34].

This technique can diagnose and identify faults that occur in three phase inverters. The proposed technique is based on the analysis of the output currents of the inverter, under normal (healthy) and faulty operation [35] .The Mamdani-type fuzzy inference system was adopted with six input variables (μ_A^+, μ_A^-, μ_B^+, μ_B^-, μ_C^+, μ_C^-) from the characteristic extraction functions and an output variable representing the state of health of the inverter considered in the study. In this fuzzy logic-based diagnosis approach, the output is the faulty switch number ($T_i = 0, \ldots, 12$).

The input quantities are normalized to a range [-1,1]. The membership functions of the inputs and outputs are depicted in Fig. 6 and Fig. 7 respectively.
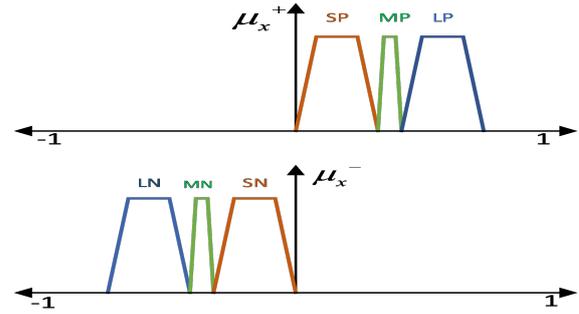

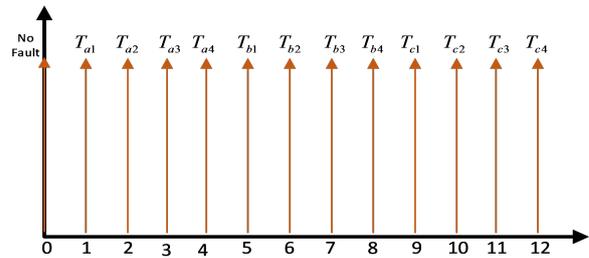**Fig. 6:** Membership functions of the inputs.

Fig. 7: Membership functions of the outputs.

3.2. Fuzzy logic rules

In general, the procedure for operating a fuzzy system is accomplished in three steps:

- The fuzzification block which converts numerical values into linguistic values using membership functions (MFs). Fuzzification provides a series of fuzzy variables, joined by a vector, which will be introduced to the inference block [36, 37].

- In the inference block, the values of the linguistic variables are linked by several rules that characterize the behavior of the system under normal operating conditions or in the presence of a fault.

- In the defuzzification block, the fuzzy values are converted back to real values that allows to infer the state of the system [36, 37].

The fuzzy rules are extracted using the relationships shown in Tab. 2. In the fuzzy logic control system, fuzzification is used to create fuzzy variables from normalized inputs (μ_x^+, μ_x^-) using MFs. The varied output levels are chosen from 0 to 12 for switch faults, which can accurately depict the number of each switch fault, with zero denoting a healthy condition.

The proposed fault diagnosis method is illustrated by Fig. 8. Which was based on using the measurement of the currents.
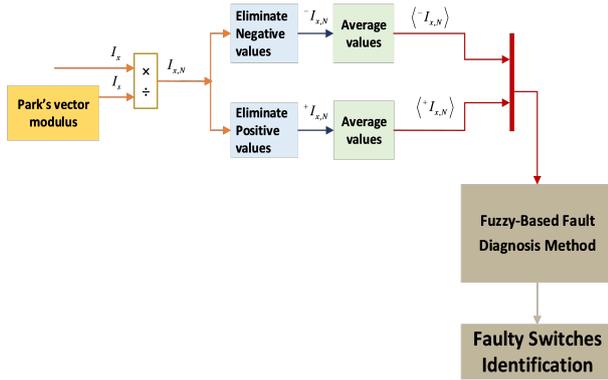
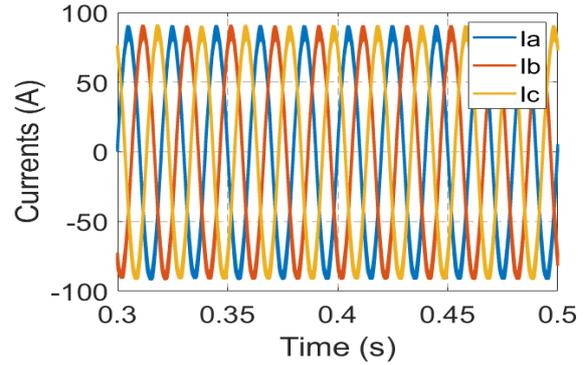**Fig. 8:** Block diagram of the proposed diagnostic method.

Fig. 10: Current generated by the GPV.

4. Simulation of the diagnosis approach

This section presents the simulation results of OCF in our PV system, as well as the performance of the proposed fault diagnosis technique. The PV system under study is simulated in MATLAB/ Simulink software. To assess the effectiveness of the proposed fault detection method, a series of simulation tests and scenarios are performed. The parameters of the grid-connected PV system are summarized in Appendix A.

Fig. 9 shows the time-varying irradiance used as input to the grid-connected PV system. The temperature was fixed at 25 ^{0}C.

Fig. 11: Power generated by the GPV.

This section introduces the simulation results obtained from the faulty operation of the grid-connected 3L inverter. These results were obtained by modeling the system in Matlab.

Specifically, an open circuit fault was generated at switch T_{a1} at time t = 1 s. The fault detection method used is presented in the previous section. Fig. 12 illustrates the three-phase currents and the output of the fault detection approach.

Fig. 12 depicts the simulation results of the three phase currents along with the diagnostic outcomes. When an OCF is introduced at t= 1s in the IGBT switch T_{a1} is introduced. The positive half-cycle of current I_a gets eliminated. As a result, the diagnostic variable μ_A^+ drops instantly, and converges to a value of approximately 0.5e-3, which is below the threshold value I_{av}^{th2+}.

For the fault diagnosis, the fuzzy fault diagnosis approach was employed using a two output fuzzy logic system to address scenarios involving multiple faults within the T-Type inverter, this enhanced methodol-
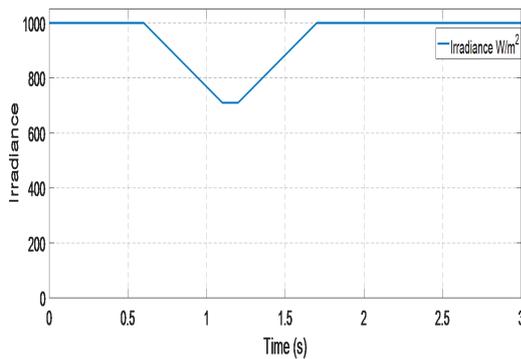

Fig. 9: Irradiance of the GPV.

Fig. 10 and Fig. 11 present the simulation results that illustrate the evolution of the current and power output of the photovoltaic panel, as obtained through the ANFIS method algorithm. As can be observed, the power of the panel accurately tracks changes in irradiation and remains stable, with only minor oscillations around the optimal power points. These results demonstrate the effectiveness of the MPPT ANFIS control.
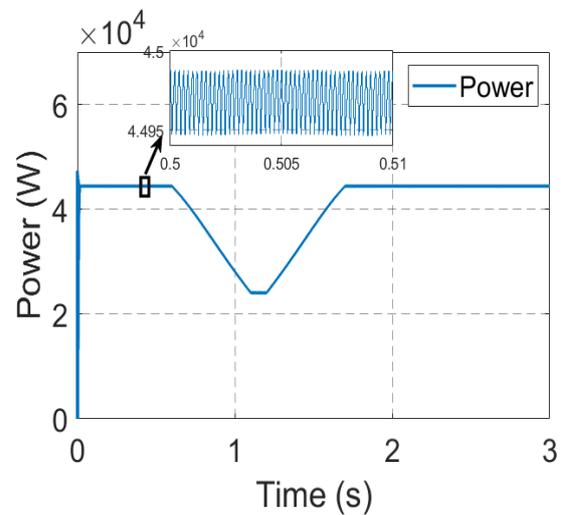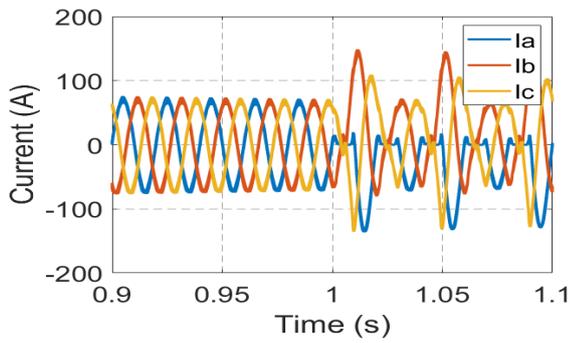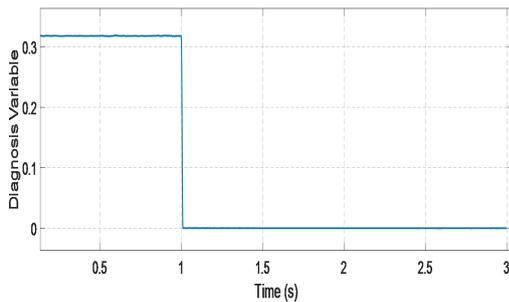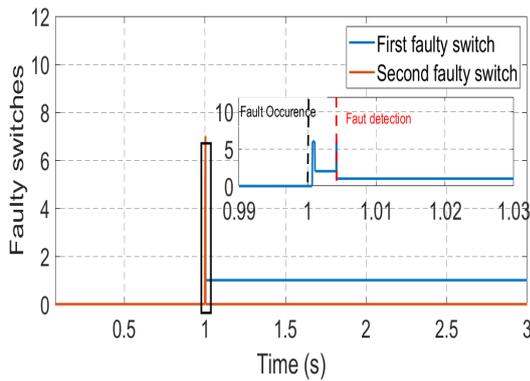
ogy allows for the simultaneous detection of multiple fault cases. Based on Fig. 12(c) the output of the fuzzy logic is the fault diagnosis signal with a magnitude of 1. the fuzzy logic output accurately reflected the presence of the single OCF, indicating a value of 1. The successful identification of the single faulty switch demonstrates the potential of the developed diagnostic approach It can already be noted that the fault is indeed detected within a half of period.
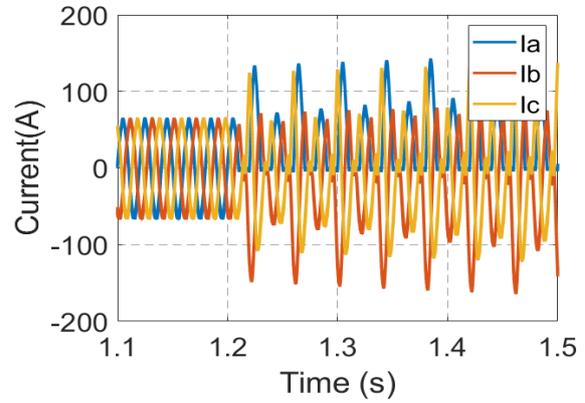
As shown in Fig. 13, when the fault occurred at t = 1.2 s, it affected the negative part of the leg A current waveform, the diagnostic variable μ_A^- rises to -0.5e-3 enabling effective identification and localization of the failure.

Fig. 12: Simulation results of the PV system under OCF in T_{a1} (a) Three Phase Currents, (b) Fault detection (c) Fault Location
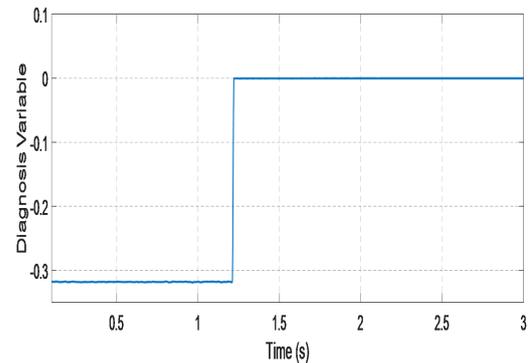
.

Fig. 13: Simulation results of the PV system under OCF in T_{a4} (a) Three Phase Currents, (b) Fault detection (c) Fault Location.

Fig. 13 shows the simulation results obtained under the fault conditions as previously simulated, an open circuit fault is applied to switch T_{a4} at time t=1.2s.
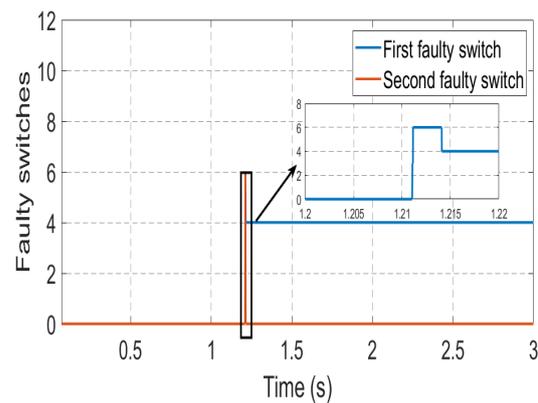
An OCF of switches T_{b3} and T_{b2} (inner switches) at t = 1.2s is simulated in Figs. 14 and 15 respectively.

Fig. 14: Simulation results of the PV system under OCF in T_{b3} (a) Three Phase Currents, (b) Fault location.

the open-circuit fault occur in one of the inner switch of the T-Type inverter. The phase current is distorted after the open fault occurs. The diagnostic variable μ_B^+ decreases immediately, and converges to a value of 0.21, which is below the threshold value I_{av}^{th1+} in the case of OCF at T_{b2}.

The simulation results obtained showed the effectiveness of the proposed fault detection method. All faults were accurately identified and classified. The proposed fuzzy diagnostic algorithm is now tested on its ability to locate faults. Previous figures show the location of different single faulty switches.

Since the percentage of three or more OCF is very low, this paper will focus also on double-switch failures. Figs. 16-17 show the scenario of two IGBTs experiencing OCFs at the same time.

The results presented here confirm that the proposed fault detection of OCF can function well during simultaneous OCFs. First, Fig. 16 which correspond to faults occurring in switches T_{a1} and T_{a4} belonging to the same inverter leg. The results show the behavior for simultaneous OCFs in the upper switch and second bottom switch.
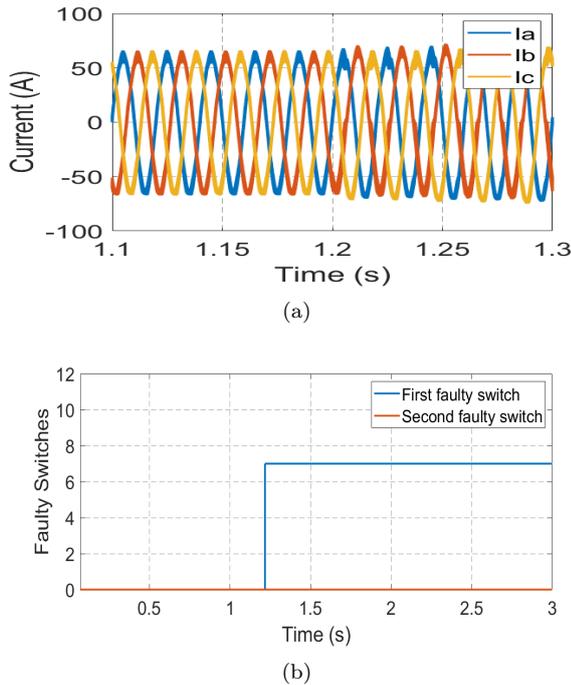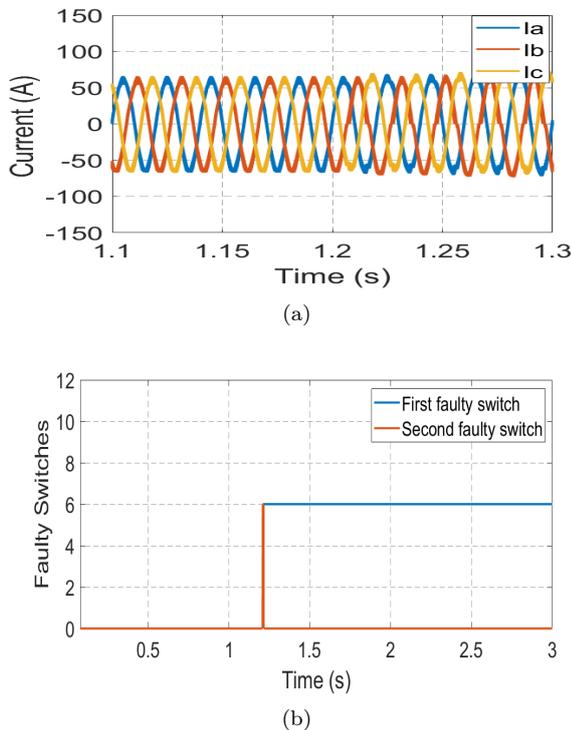

Fig. 15: Simulation results of the PV system under OCF in T_{b2} (a) Three Phase Currents, (b) Fault location.

Fig. 14 and Fig. 15 show the wave-forms of the simulation results when the switches T_{b3} and T_{b2} are open-circuited, respectively. It can be seen that when
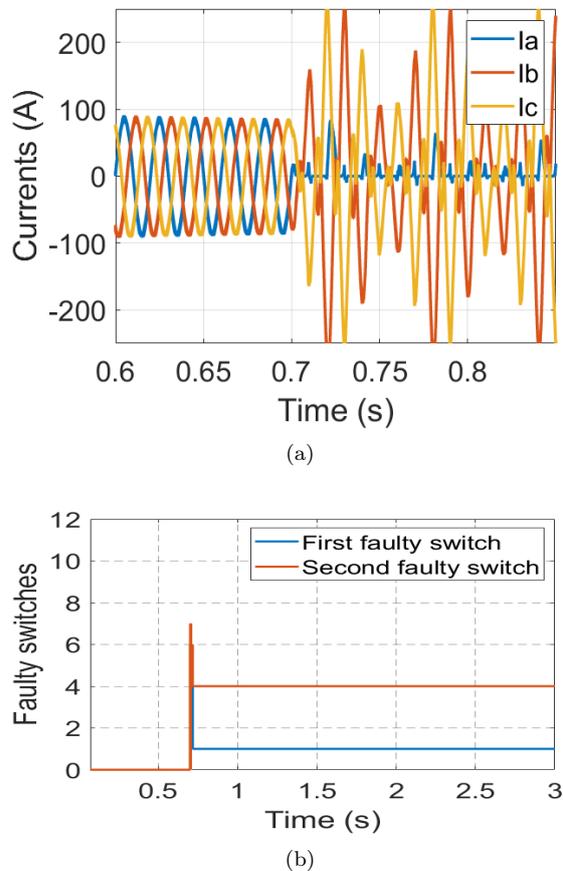

Fig. 16: Simulation results of the PV system under OCF in T_{a1} and T_{a4} (a) Three Phase Currents, (b) Fault location.

At t = 0.7s, the OCF in IGBT T_{a4} is applied to the fault in T_{a1}, the diagnostic variable μ_A^+ instantly falls to 0.5e-3 and falls below the threshold I_{av}^{th2+}. When the second fault in T_{a4} is added, the second diagnostic variable μ_A^-, rises to -0.5e-3 which allow for effective identification and location of both failures.

For our developed fuzzy logic-based diagnostic approach, we simulated a scenario involving the occurrence of two simultaneous faults within the same leg of the T-Type inverter. Notably, our method successfully detected both faults, as evidenced by the outcomes observed in the diagnostic outputs. Specifically, the first diagnostic output responded with a value of 1 indicative of the detection of the initial fault, while the second diagnostic output exhibited a value of 4 corroborating the successful identification of the second concurrent fault. This outcome validates the robustness and efficacy of our fuzzy logic approach in addressing multiple fault scenarios.

In this instance, both the top switch T_{a1} in phase A and the bottom switch of phase B T_{b4} are open circuited. The detection and localization algorithm of two simultaneous IGBTs open circuit fault is carried out. The phases currents are shown in Fig. 17.
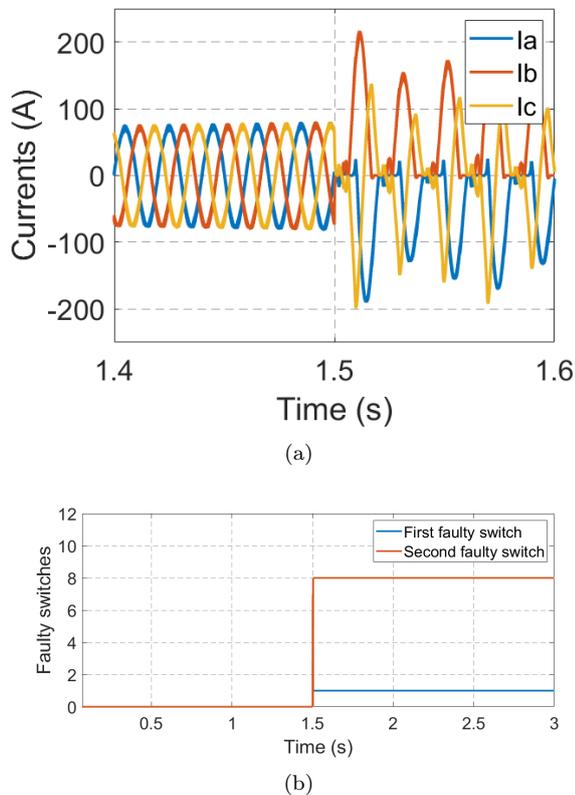
Fig. 17 depicts the simulation results for the three phase currents, as well as the fuzzy logic output. At the time t = 1.5 s, the gate signals of the IGBT's T_{a1} and T_{b4} are open circuited, resulting in failure of an open-circuit in the first phase A and in phase B. It is evident that the suggested fault diagnostic algorithm has the ability to identify and localize the problem in a single crucial period at a variety of fault types and locations.

5. Conclusion

This paper focuses on the identification and diagnosis of power switch open circuit fault in a 3L T-Type inverter in PV system. The proposed approach is based on the extraction and analysis of averaged positive and negative parts of the normalized currents. The performance of the extracted features is analyzed under both healthy and defective conditions in order to establish the fuzzy bases and derive the rules of the recommended fuzzy logic detection approach. The results of the case study under consideration demonstrate to the effectiveness of the suggested detection method in precisely locating the faulty switch and identifying the numerous faulty combinations situations. The simulation results show that the proposed fuzzy based fault diagnosis approach is very effective in identifying single and multiple open-circuit faults in the power switches. This study suggests several possibilities for future research. Using advanced machine learning for more accurate and efficient method of diagnosis which can be tested on different topologies of inverters. Moreover, transitioning from simulation-based verification to real-hardware implementation would facilitate the validation of the method's reliability and practicality.

Author Contributions

The idea for this paper was conceived by A.M. and S.L., with S.L. supervising the work. A.M. and A.A.B. collaborated on the design of the OCF diagnosis for the inverter and the formulation of the research diagnosis method. A.M. contributed to the writing of the manuscript, while S.L., T.A., and M.S. provided crucial feedback and approved the final version for submission.

Fig. 17: Simulation results of the PV system under OCF in T_{a1} and T_{b4} (a) Three Phase Currents, (b) Fault location.

References

[1] SHEIKH AHMADI, S.H, M. KARAMI, M. GHO-LAMI and R. MIRZAEJ. Improving MPPT Performance in PV Systems Based on Integrating the Incremental Conductance and Particle Swarm Optimization Methods. *Iranian Journal*

of Science and Technology, Transactions of Electrical Engineering. 2022, vol. 46, pp. 27–39. DOI: 10.1007/s40998-021-00459-0.

[2] KOLLIMALA, S and M. MISHRA.A Novel Adaptive P&O MPPT Algorithm Considering Sudden Changes in the Irradiance. IEEE Transactions on Energy Conversion. 2014, vol. 29,pp. 602–610. ISSN 1804-3119. DOI: 10.1109/TEC.2014.2320930.

[3] KHALEEL, M.M, M.R. Adzman, and S. M. Zali. An integrated of hydrogen fuel cell to distribution network system: Challenging and opportunity for D-STATCOM. Energies.2021, vol. 14, no. 21, pp. 7073, 2021. DOI: 10.3390/en14217073.

[4] KHALEEL, M.M. T. MOHAMED GUENDOURI. A. ALI AHMED. A. ALSHARIF and all. Impact of mechanical storage system technologies: A powerful combination to empowered the electrical grids application. 2022 IEEE 2nd International Maghreb Meeting of the Conference on Sciences and Techniques of Automatic Control and Computer Engineering. Sabratha, Libya: IEEE, 2022,pp. 628–636. DOI: 10.1109/MI-STA54861.2022.9837670.

[5] NASIRI, M., S. CHANDRA, M .TAHERKHANI and S.J. MCORMAK. Impact of Input Capacitors in Boost Converters on Stability and Maximum Power Point Tracking in PV systems. In: 48th Photovoltaic Specialists Conference. Fort Lauderdale, USA: IEEE, 2021. ISBN 0160-8371. DOI: 10.1109/PVSC43889.2021.9518903.

[6] MOHAMED, S and M. ABD ELSATTAR. A comparative study of P&O and INC maximum power point tracking techniques for grid-connected PV systems. SN Appl. 2019, vol. 01,pp. 174. DOI: 10.1007/s42452-018-0134-4.

[7] NASIR, A., A. RASOOL., D. SIBTAIN and all. Adaptive Fractional Order PID Controller Based MPPT for PV Connected Grid System Under Changing Weather Conditions. J. Electr. Eng. Technol. 2021, vol. 16,pp. 2599—2610. DOI: 10.1007/s42835-021-00782-w.

[8] ALY, M and H. REZK. An Efficient Fuzzy Logic Fault Detection and Identification Method of Photovoltaic Inverters. Computers Materials and Continua. 2021, vol. 64,pp. 1546—2226. DOI: 10.32604/cmc.2021.014786.

[9] ALY, M., H, AHMED and M, SHOYAMA. Developing new lifetime prolongation SVM algorithm for multilevel inverters with thermally aged power devices. IET Power Electronics. 2017, vol. 10,pp. 2248—2256. DOI: 10.1049/iet-pel.2017.0327.

[10] MA, K., D, ZHOU and F, BLAABJERG. Evaluation and Design Tools for the Reliability of Wind Power Converter System. Journal of Power Electronics. 2015, vol. 15,no. 5,pp. 1149—1157. DOI: 10.6113/JPE.2015.15.5.1149.

[11] SALEM, A., M.A, ABIDO. T-Type Multilevel Converter Topologies: A Comprehensive Review.Arab J Sci Eng.2019, vol. 44,pp. 1713—1735. DOI: 10.1007/s13369-018-3506-6

[12] SATTI, A., A. HASSAN and M. AHMAD. A New Multilevel Inverter Topology for Grid-Connected Photovoltaic Systems. International Journal of Photoenergy.2018, vol. 2018, Article ID 9704346, 9 pages. DOI: 10.1155/2018/9704346

[13] ALTIN, N., I, SEFA., H, Komurcugil and S, OZDEMIR. Three-phase three-level T-type grid-connected inverter with reduced number of switches. 6th International Istanbul Smart Grids and Cities Congress and Fair. Istanbul:IEEE,2018. DOI: 10.1109/SGCF.2018.8408942

[14] ZORIG, A., M, BELKHEIRI., S, BARKAT. Control of three-level T-type inverter-based grid connected PV system.13th International Multi-Conference in Systems, Signals and Devices. Leipzig, Germany:IEEE, 2016. DOI: 10.1109/SSD.2016.7473723.

[15] CHEN, D., Y, LIU., S, ZHANG. Open-circuit fault diagnosis method for the T-type inverter based on analysis of the switched bridge voltage. IET Power Elctronics.2019, vol. 12, pp. 295–302. DOI: 10.1049/iet-pel.2018.5377.

[16] DANJIANG, C., L, YUTIAN, Z, SHOAZHONG.Fault diagnosis of T-type three-level inverter based on bridge voltages.Archives of Electrical Engineering. 2021, vol. 70, pp. 73–87. DOI:10.24425/aee.2021.136053.

[17] WANG, B., Z, LI, Z, BAI., P.T, KREIN and H, MA.Real-time diagnosis of multiple transistor open-circuit faults in a T-type inverter based on finite-state machine model.CPSS Transactions on Power Electronics and Applications. 2020, vol. 5, pp. 74–85. DOI:10.24295/CPSSTPEA.2020.00007.

[18] CHOI, U.M., K.B, LEE and F, BLAABJERG.Diagnosis method of an open-switch fault for a grid-connected T-type three-level inverter system.3rd IEEE International Symposium on Power Electronics for Distributed Generation Systems. 2012, Aalborg, Denmark:IEEE. DOI:10.1109/PEDG.2012.6254044.

[19] CHOI, U.M., K.B, LEE and F, BLAAB-JERG.Diagnosis and Tolerant Strategy of an Open-Switch Fault for T-Type Three-Level Inverter Systems.*IEEE Transactions on Industry Applications*. 2014, vol. 50, pp. 495–508. DOI:10.1109/TIA.2013.2269531.

[20] CHOI, U.M and K.B, LEE.Detection method of an open-switch fault and fault-tolerant strategy for a grid-connected T-type three-level inverter system.*2012 IEEE Energy Conversion Congress and Exposition (ECCE)*. 2012, Raleigh, NC, USA:IEEE. DOI:10.1109/ECCE.2012.6342254.

[21] HE, J., N, DEMERDASH, N, WEISE., R, KATEBI.A Fast On-Line Diagnostic Method for Open-Circuit Switch Faults in SiC-MOSFET-Based T-Type Multilevel Inverters.*IEEE Transactions on Industry Applications*. 2017, vol. 53, pp. 2948–2958. DOI:10.1109/TIA.2016.2647720.

[22] HU, H., F, FENG and T, WANG. Open-circuit fault diagnosis of NPC inverter IGBT based on independent component analysis and neural network.*2020 7th International Conference on Power and Energy Systems Engineering*. 2020, Fukuoka, Japan:Energy Reports.DOI:10.1016/j.egyr.2020.11.273.

[23] WAN, X., H, HU and Y, YU. Open-circuit Fault Diagnosis for Grid-connected NPC Inverter based on Independent Component Analysis and Neural Network.*TELEKMNIKA*. 2017, vol. 15, pp. 36–47. DOI:10.12928/TELKOMNIKA.v15i1.3677.

[24] BENGHARBI, A.A., S, LARIBI, T, ALLAOUI and A, MIMOUNI. Photovoltaic system faults diagnosis using discrete wavelet transform based artificial neural networks.*Electrical Engineering and Electromechanics*. 2022, vol. 6, pp. 42–47. DOI:10.20998/2074-272X.2022.6.07.

[25] MIMOUNI, A., S, LARIBI, M, SEBAA, T, AL-LAOUI AND A.A. BENGHARBI. Fault diagnosis of power converters in a grid connected photovoltaic system using Artificial Neural Networks.*Electrical engineering and electromechanics*. 2023, vol. 1, pp. 4–10. DOI:10.20998/2074-272X.2023.1.04.

[26] KHAMIS, A., M, RUDDIN, A, GHANI and all.Control Strategy for Distributed Integration of Photovoltaic and Battery Energy Storage System in Microgrids.*TELEKOMNIKA*. 2018, vol. 5, pp. 2415–2427. DOI:10.12928/telkomnika.v16i5.10249.

[27] IBRAHIM, I.A., T, KHATIB, A, MOHAMED and W, ELMENREICH.Modeling of the output current of a photovoltaic grid-connected system using random forests technique.*Energy Exploration and Exploitation*. 2018, vol. 36, pp. 132–148. DOI:10.1177/0144598717723648.

[28] YAQOOB, S., A, SALEH, S, MOTAHHIR and all. Comparative study with practical validation of photovoltaic monocrystalline module for single and double diode models.*Sci Rep*. 2021, vol. 11, pp. 21822. DOI:10.1038/s41598-021-01357-5.

[29] GHAYTH, A., Z, Yusupov and M, Khaleel. Performance Enhancement of PV Array Utilizing Perturb and Observe Algorithm. *International Journal of Electrical Engineering and Sustainability (IJEES)*.2023, vol. 1, no. 2,pp. 29–37. DOI:ijees.org/index.php/ijees/article/view/33.

[30] KHALEEL, M., Yusupov, Z., Yasser, N., and J. El-Khozondar, H. Enhancing Microgrid Performance through Hybrid Energy Storage System Integration: ANFIS and GA Approaches. *International Journal of Electrical Engineering and Sustainability (IJEES)*.2023, vol. 1, no. 2, pp. 38–48. DOI:ijees.org/index.php/ijees/article/view/34.

[31] GUENOUNOU, O., B, DAHHOU and F, CHABOUR.Adaptive fuzzy controller based MPPT for photovoltaic systems.*Energy Conversion and Management*. 2014, vol. 78, pp. 843–850. DOI:10.1016/j.enconman.2013.07.093.

[32] REZK, H., M, ALY, M, AL-DHAIFALLAH and M, SHOYAMA.Design and Hardware Implementation of New Adaptive Fuzzy Logic-Based MPPT Control Method for Photovoltaic Applications.*IEEE Access*. 2019, vol. 7, pp. 106427 – 106438. DOI:10.1109/ACCESS.2019.2932694.

[33] MTEPELE, K., D, CAMPOS DOLGADO, A, VALDEZ FERNANDEZ and J, PECINA SANCHEZ. Model-based strategy for open-circuit faults diagnosis in n-level CHB multilevel converters.*IET Power Electronics*. 2019,vol. 12,no. 4 pp. 648-655. DOI:https://doi.org/10.1049/iet-pel.2018.5478.

[34] LARIBI, S., M, BENDIABELLAH, M, YOUCEF and S, MERADI.Use of neuro-fuzzy technique in diagnosis of rotor faults of cage induction motor.*5th International Conference on Electrical Engineering*. 2017,BOUMERDAS, ALGERIA:IEEE. DOI:10.1109/ICEE-B.2017.8192148.

[35] LARIBI, S., M, BENDIABELLAH and S, MERADI. Fault diagnosis of rolling element bearings using artificial neural network.*International Journal of Electrical and Computer Engineering*. 2020, vol. 10, no. 5, p. 5288–5295. DOI:10.11591/ijece.v10i5.pp5288-5295.

[36] SHETGAONKAR, S.Fault diagnosis in induction motor using fuzzy logic.*2017 International Conference on Computing Methodologies and Communication.* 2017, Erode, India:IEEE. DOI:10.1109/ICCMC.2017.8282693.

[37] MEHTA, P., S, SAHOO and H, DHIMAN. Open Circuit Fault Diagnosis in Five-Level Cascaded H-Bridge Inverter.*International Transactions on Electrical Energy Systems.* 2022, vol. 2022, pp. 13. DOI:10.1155/2022/8588215.

About Authors

Amina MIMOUNI (corresponding author) was born in Algeria, in 2019 she received the Engineer degree in electrical engineering from Higher School of Applied Sciences–Tlemcen,Algeria. She is currently working toward the PhD degree in L2GEGI laboratory in Ibn khaldoun University, Algeria. Her research interests include, Renewable Energy, Fault diagnosis in power converters.

Souad LARIBI was born in Algeria, received her Ph.D. degrees in Electrical Engineering from the University of Sciences and Technology of Oran Mohamed Boudiaf (USTOMB), Oran, Algeria, in 2016 she receives her Habilitation degrees from the University Ibn Khaldoun Tiaret, Algeria, in 2020 in Electrical Engineering. Currently she working Senior Lecturer at Université Ibn Khaldoun Tiaret Algeria. Her fields of interest are electrical machines associated with static converter, control, modeling, and diagnosis and renewable energy systems. She is a member in Energetic Engineering

Tayeb ALLAOUI was born in Tiaret, Algeria. He received the diploma of Electrotechnical Engineering degree from Ibn Khaldoune University of Tiaret, Algeria. The Master degree, from the University of Science and Technology of Oran, Algeria.in 2002. The PhD degrees from the University of Science and Technology of Oran, Algeria, in 2007. His research activities are mostly concentrated in the study of power systems, FACTS, Renewable and Sustainable Energy, power management and research activities focusing a smart grid system.

Morsli SEBAA was born in Algeria, he received the magister degree in automatic control from National Higher Technical School of Oran (Algeria), and PhD degree in control engineering from University of Science and Technology of Oran (Algeria). He is now a teacher of electrical engineering at the University Ibn Khaldoun of Tiaret (Algeria) and a member in the Laboratory of Energetic Engineering and Computer Engineering (L2GEGI) at Ibn Khaldoun University of Tiaret, Algeria. His major research interests are on application of artificial intelligence and robust control techniques of process.

Abdelkader Azzeddine BENGHARBI was born in Algeria, received his BSc degree in Electrotechnical Engineering and his MSc in renewable energies on Electrotechnique Engineering from Djelfa University, Algeria. He is currently a PhD student at Tiaret University. He is also a member of the Energetic Engineering and Computer Engineering Laboratory (L2GEGI) at the same university. His research interests include renewable energy systems, electrical machines, power systems, diagnosis, control and artificial intelligence.

Appendix A   Grid connected PV system parameters.

Quantity	Value
Maximum power (W)	45032.175
Voltage at (Maximum power) (V)	394.5
Current at (Maximum power) (A)	114.15
Open circuit voltage (V)	493.5
Short circuit current (A)	123.15
V_{dc} (V)	800
C_{pv}	100 x 10-6
L	5 x 10-3
Switching frequency of the boost (Hz)	5000
Switching frequency of the inverter (Hz)	10000
Grid frequency (Hz)	50
Grid line voltage (V)	400